Synthesis and Assembly of mRNA-Bifunctional Lipid Nanoparticle (BLNP) for Selective Delivery of mRNA Vaccines to Dendritic Cells

Chen-Yo Fan,† Szu-Wen Wang,† Jia-Yan Chen,† and Chi-Huey Wong*,†,‡

†Genomics Research Center, Academia Sinica, Taipei 115, Taiwan

‡Department of Chemistry, The Scripps Research Institute, La Jolla, CA 92037

*E-mail: wong@scripps.edu

ABSTRACT: The fight against COVID-19 pandemic has gained a strong consensus about the importance of developing mRNA vaccines to rapidly respond to an outbreak. Several studies have shown that mRNA vaccines formulated as mRNA-lipid nanoparticles (LNPs) for vaccination can elicit a robust and efficient immune response. In this study, we report the preparation of mRNA-bifunctional lipid nanoparticles (mRNA-BLNPs) as vaccines for targeted delivery to dendritic cells (DCs) to improve safety and enhance immune response. Using this DC-targeted delivery system, mice immunized with SARS-CoV-2 spike mRNA-BLNP vaccine elicited a stronger immune response with higher titer of neutralizing IgG antibody response than the LNP-formulated vaccine against SARS-CoV-2. In addition, the spike mRNA-BLNP vaccine with deletion of glycosites in the stem elicited a broadly protective immune response against SARS-CoV-2 and variants. These findings suggest the importance and potential of developing DC-targeted mRNA vaccines to elicit broadly protective immune responses against human viruses.

Introduction

The outbreak of SARS-CoV-2 in 2019 that caused a global pandemic had stimulated a great deal of efforts to develop safe and effective vaccines to contain the pandemic. While many vaccine candidates have been investigated,[1] the extraordinary speed in development of effective mRNA vaccines for immunization demonstrated the powerful application of this breakthrough vaccination to control the spread of pandemics.[2-5] The success of mRNA vaccines depends on the flexible and fast design of stable mRNA sequence with nucleotide modification and subsequent manufacture of products for encapsulation in lipid nanoparticles (LNPs). The currently approved mRNA vaccines[4-5] were generated by the mRNA encoding full length spike protein with two proline substitutions to stabilize the prefusion state and formulated with a mixture of lipid carriers composed of four components, including a ionizable lipid, a phospholipid, a cholesterol and a PEG-conjugated lipid.[6]

mRNA-based vaccines are attractive because they retain similar appealing characteristics of DNA-based vaccines and offer additional benefits, such as rapid translation to the corresponding protein antigen in the cytoplasm after immunization[7-8] and providing adjuvant activities via toll-like receptors (TLRs) to enhance immune response.[7] The success of mRNA-based vaccines against SARS-CoV-2 has stimulated interests in developing new mRNA vaccines against other diseases, particularly infectious diseases and cancers and new methods for stabilization and targeted delivery of mRNA[9] to improve efficacy and safety.[10-13] Among the mRNA delivery systems, non-viral vectors represent a simpler, more flexible and safer alternative to viral vectors, in addition to simple quantitative production and low immunogenicity. With the advances in development of new biocompatible

materials and innovative fabrication approaches, non-viral vectors have become the preferred vehicles for mRNA delivery and a variety of non-viral vectors have been explored, including lipids and polymers.[14-15]

However, recent attention has been focused on development of lipid nanoparticles for encapsulation of nucleic acids to reduce their degradation by nucleases and provide better transfection efficiency than other delivery systems.[16] Furthermore, LNPs can be modified to target specific subsets of antigen-presenting cells (APCs) to improve efficacy and safety, making LNPs more suitable for mRNA vaccine formulation.[17] Muscle cells, for example, have been shown to be involved in the presentation of RNA and DNA vector encoded antigens.[18] Therefore, selective delivery of an mRNA vaccine to APCs will enhance CD4 and CD8 immune responses and minimize undesirable translation of mRNA in different cells. In addition, the cross presentation by APCs of myocyte-derived antigens has been demonstrated to be the primary mechanism for priming CD8 T cells.[19] All these studies point to the need to develop APC-targeted mRNA vaccines with enhanced immune response.[20]

A major component of BLNP used in this study was the bifunctional glycolipid C34, which was designed to target the CD1d receptor on dendritic cells (DCs) and the T cell receptor on iNKT cells to release interferon-γ (IFN-γ) and IL-4 to balance the Th1 and Th2 pathways and induce $CD4^+$ and $CD8^+$ T cell responses.[21,26]

In addition, we modified the glycan moiety of C34 to mannose and took the advantageous bifunctional properties of C34[27-28] with mannose head and lipid tail designed to target dendritic cell (DC) and developed a new LNP formulation with simpler compositions for selective mRNA delivery. The mRNA is first encapsulated with the lipid mixture to generate mRNA-BLNP and protect the mRNA from RNase attack and efficiently delivered the encapsulated mRNA to DCs for internalization and release of mRNA for antigen translation and presentation. Here, the spike-mRNA of SARS-CoV-2 was encapsulated with the lipids to form mRNA-BLNP and immunized in mice. Analysis of immune responses showed that the spike mRNA-BLNP vaccine elicited higher levels of spike protein-specific neutralizing antibodies than the traditional mRNA-LNP vaccine. In addition, the mRNA-BLNP vaccine with deletion of glycosites in the stem elicited enhanced and broadly protective antibody and CD8+ T-cell responses to SARS-CoV-2 variants.

Result and Discussion

One of the major advantages of using synthetic vectors for delivery of mRNA is the flexibility in size, structure and composition. In our first approach, we reduced the four-component LNP commonly used in mRNA formulation to a two-component lipid nanoparticle to simplify the formulation process, including a guanidinyl lipid and a zwitterionic lipid to form mRNA-GZ-LNP (figure 1). In general, LNPs include a helper lipid and a cationic lipid. The helper lipid was used to stabilize the mRNA-LNP delivery system, such as 1,2-dioctadecanoyl-sn-glycero-3-phosphocholine (DSPC)[29] or 1,2-dioleoyl-sn-glycerol-3-phosphoethanolamine (DOPE).[30] These helper lipids not only stabilize the particles but also enhance mRNA delivery efficiency.[31]

Ionizable lipids are of great importance for the encapsulation and delivery of mRNAs because their positively charged head groups can interact with the negatively charged phosphate backbone of the mRNA molecule.[32] Besides, protonation of the ionizable components destabilizes the anionic vesicular membrane and facilitates nanoparticle disassembly, leading to the release of mRNA to the cytosol.[33] To facilitate the mRNA encapsulation and delivery, the ionizable lipid is the most

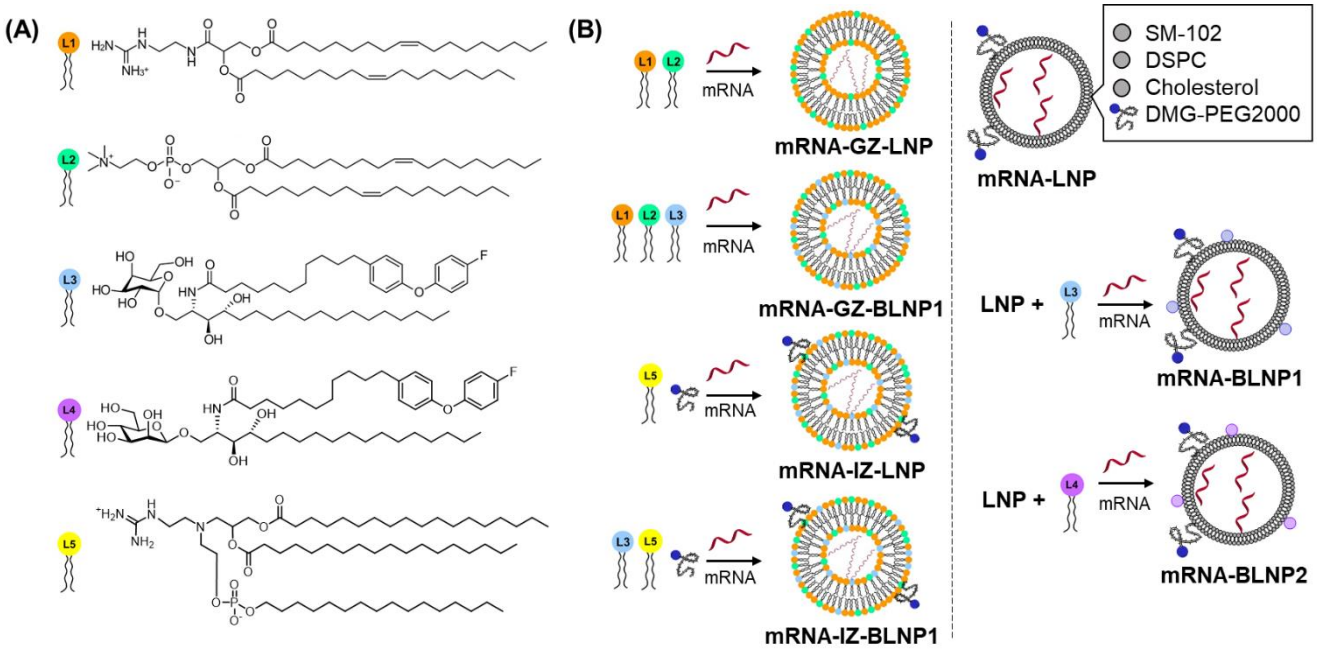

Figure 1. (A) Structure of synthetic lipids (B) constructs of different mRNA-LNP and mRNA-BLNP preparations with bifunctional lipid for DC-targeted delivery.

abundant component in LNP formulation. However, the phosphate group with negative charge in helper lipid allows selective delivery to the spleen, and efficiently mediated protein expression in spleen and lymph nodes.[34] This property prompted us to introduce a higher number of zwitterion groups into the formulation of mRNA-LNPs to ensure a more precise mRNA delivery. By connecting a guanidine head with a tertiary amine and a phosphate group in one molecule, the guanidine group is positively charged at physiological and acidic conditions and the phosphate group is negatively charged at physiological condition and neutral at acidic condition. The combination of these functional groups increased the overall phosphate ingredient in IZ lipid nanoparticles (IZ-LNP) to facilitate targeting.

Moreover, in our aim of developing new lipids for selective delivery of mRNA-LNP to dendritic cells, we include the bifunctional lipid L3 in the mRNA-GZ-LNP, mRNA-IZ-LNP and mRNA-LNP formulation for targeting CD1d receptor on dendritic cells. Using these LNPs, we can synthesize nanoparticles in size of one to two hundred nm with high transfection efficiency in HEK293 cells (Figure S1).

Although it is practical to use these LNP formulation systems for *in vitro* or *in vivo* study, the long-term storage and serum instability of these LNPs was still a concern due to the absence of cholesterol and PEGylated lipids. When mRNA-GZ-BLNP1 was incubated with 10% FBS at 37 °C for 6-48 h, we found a gradual increase of particle size as the incubation time increased (figure S2). Interestingly, inclusion of L3 showed a slightly stabilization of LNP, while inclusion of cholesterol and PEGylated lipid improved the transformation of LNPs to multilayer nanoparticles. Therefore, for *in vivo* studies such as intravenous injection, 1.5% PEG lipid and 38.5% cholesterol were included in mRNA-GZ-BLNP1 or mRNA-IZ-BLNP1 to improve stability.

In the assembly of mRNA with GZ-LNP/IZ-LNP and mRNA mixing with L3, we observed an average particle size of mRNA-

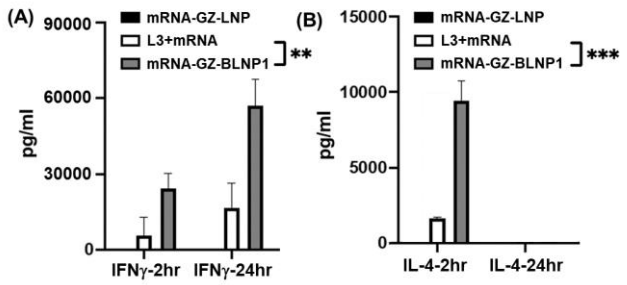

Figure 2. The humoral immune response induced by different formulations of mRNA-LNPs. (A) IFN-γ induced by L3+mRNA or mRNA-GZ-BLNP1 (B) IL-4 induced by L3+mRNA or mRNA-GZ-BLNP1. Cytokines were analyzed in mice serum at 2 and 24 hr after immunization.

GZ-BLNP1 or mRNA- IZ-BLNP1 at around 174 or140 nm by DLS, respectively with spherical morphology revealed by TEM and CryoEM (Figure S3).

We then immunized mice with spike-encoding mRNA-LNPs and evaluated their immune responses. To assess the adaptive immune response to the mRNA-GZ-LNP and mRNA-GZ-BLNP1, analysis of IFN-γ and IL-4 concentrations in sera at various time points after the first immunization was done by ELISA. Mouse sera collected at 2 and 24 h after injection of L3+mRNA showed induction of IL-4 and IFN-γ. Surprisingly, mRNA-GZ-BLNP1 triggered the secretion of cytokines IL-4 and IFN-γ at 2 h and induced a significantly higher level of cytokines as compared to the L3+mRNA group. In addition, the IFN-γ concentration dramatically increased after 24 h treatment compared to the L3+mRNA group (figure 2A). For IL-4, the mRNA-GZ-BLNP1 vaccine stimulates IL-4 production about five times higher than L3+mRNA after 2 h treatment (Figure 2B). Notably, the induction of IFN-γ and IL-4 was only attributed to the treatment with addition of L3. mRNA-GZ-LNP alone did not induce any release of cytokines, however, mRNA-GZ-BLNP1 stimulated enhanced production of the Th2 cytokine IL-4 and Th1 cytokine IFN-γ as compared to L3+mRNA.

We next evaluated the effect of WT spike encoding mRNA-BLNP vaccination. BALB/c mice were immunized with the vaccines on

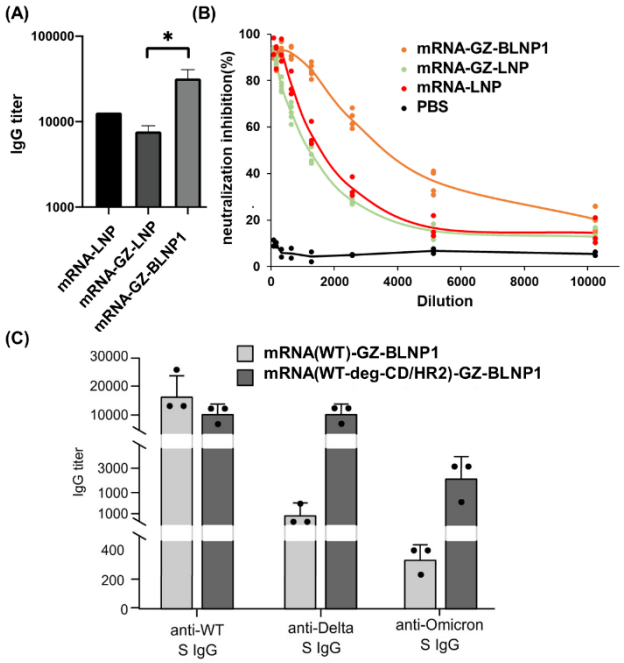

Figure 3. (A) IgG titer and (B) pseudovirus-based neutralization assay of mRNA-LNP, mRNA-GZ-LNP, and mRNA-GZ-BLNP1. Mice were immunized at day 0 and day 14 and the sera were collected at day 21. (C) IgG titers of sera from mice immunized with mRNA(WT)-GZ-BLNP1 or mRNA(WT-deg-CD/HR2)-GZ-BLNP1 with deletion of glycosites in stem against WT, Delta and Omicron spike proteins.

day 0 and received a boost on day 14. Although the levels of IgG titers were slightly lower in the group receiving mRNA-GZ-LNP compared to mRNA-LNP, we observed a six-fold enhancement of anti-spike antibodies from the sera of mRNA-GZ-BLNP1 immunized mice (Figure 3A). The serum was then tested for the ability to neutralize pseudovirus-mediated entry to the ACE2-expressing cells. While the level of antisera from mice immunized with mRNA-GZ-LNP was similar to the mRNA-LNP group, there is a significantly higher level of neutralizing antibodies in the mRNA-GZ-BLNP1 group (Figure 3B). Besides, the IgG titers of mice immunized with

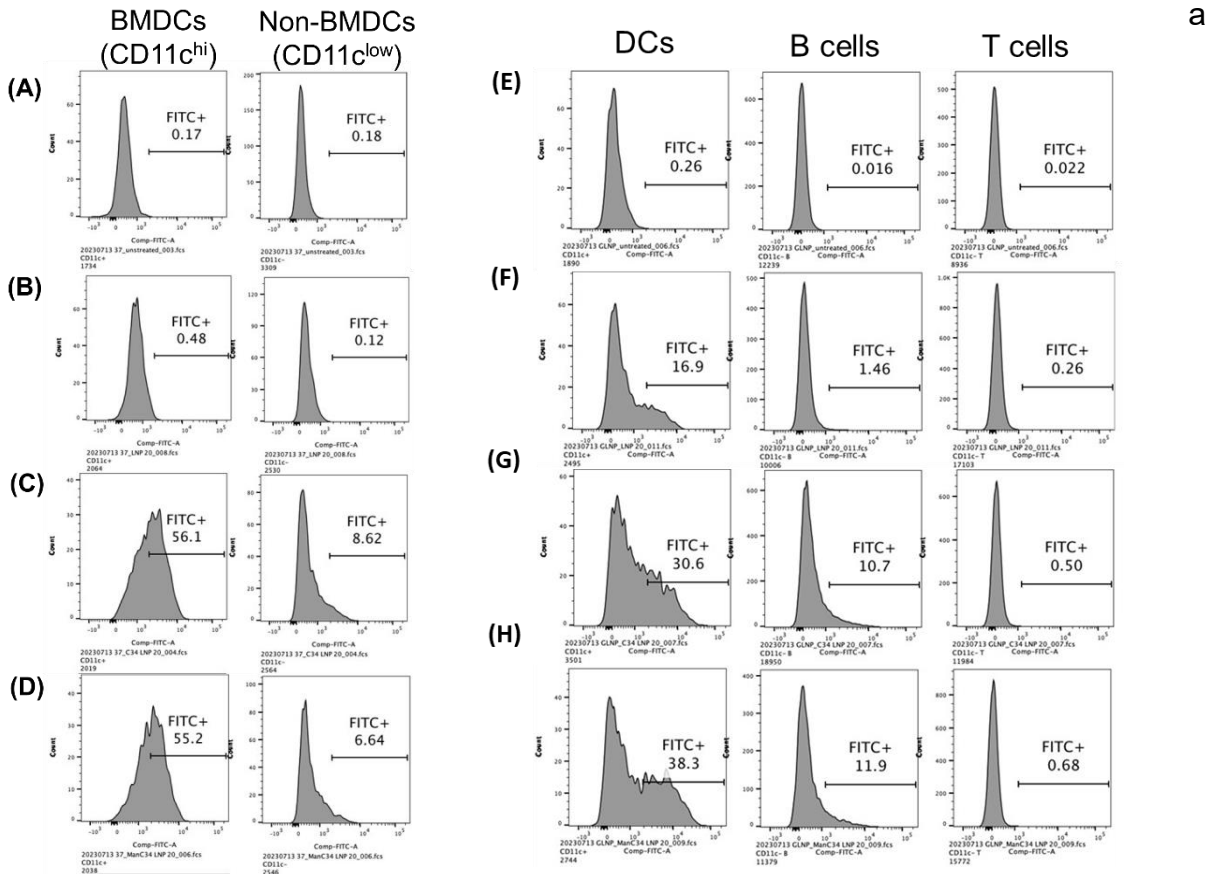

Figure 4. Cellular uptake by BMDCs and non-BMDCs by (A)(E) no mRNA-LNP treated (B)(F) FITC-labeled mRNA-LNP (C)(G) FITC-labeled mRNA-BLNP1 (D)(H) FITC-labeled mRNA-BLNP2.

mRNA-GZ-BLNP1 against WT, Delta and Omicron spike protein were also determined to investigate whether removing the glycosites on CD/HR2 domain provided a better protection against SARS-CoV-2 variants. Figure 3C showed that the WT mRNA vaccine induced a high IgG titer against WT spike protein, but the IgG titer decreased against Delta and Omicron spike protein. Although the mRNA (WT-deg-CD/HR2)-GZ-BLNP1 vaccine induced a comparable IgG titer against WT spike protein compared to mRNA(WT)-GZ-BLNP1, the mRNA(WT-deg-CD/HR2)-GZ-BLNP1 vaccine induced a better IgG titer against Delta and Omicron spike protein compared to mRNA(WT)-GZ-BLNP1.

On the other hand, we combined our bifunctional lipid to the current LNP formulation (Figure 1B) and evaluated the practical use of bifunctional lipid in the lipid-based delivery system. As shown in Figure S4, we observed strong induction of both cytokines IL-4 and IFN-γ when L3 was introduced into the LNP.

In addition, we assess CD1d-mediated binding and uptake of the mRNA vaccine formulated with the bifunctional lipid-incorporated LNP using BMDCs from mice. BMDCs expressed CD1d and equivalent level of CD11c as marker. Flow cytometry analysis of BMDCs revealed that the mRNA-LNP containing the CD1d-binding ligand L3 showed a selective uptake by BMDCs and not by the non-BMDCs cells (figure 4C). Control FITC-mRNA-LNP without L3 showed no uptake by BMDCs and non-BMDCs (figure 4B). The other mRNA-BLNP2 with Man-C34-incorporated also showed a similar phenomenon observed in mRNA-BLNP1 vaccine (figure 4D), indicating that the BMDCs uptake was mediated by the glycolipid with galactose or mannose head. In the other study, the prepared mRNA-LNPs were incubated in DCs, B cells, and T cells, and we found that mRNA-BLNP1

and mRNA-BLNP2 showed a high preference to DCs compared to B cells and T cells. Among them, mRNA-BLNP2 with 38.3% FITC positive was probably attributed to the dual-targeting to DCs by CD1d receptor and mannose receptors.

We also examined the feasibility of spike mRNA formulated with L3-containing LNP with regard to spike-specific antibody response in the serum. The result indicated that mRNA-BLNP1 exhibited a remarkable immunogenicity and pseudovirus neutralization after second immunization on day 14, with 4-fold increase in titer compared to mRNA-LNP on day 21 (figure S5). We confirmed that the addition of bifunctional lipid into the mRNA-LNP vaccine elicited an enhanced and robust antigen-specific immune response.

Conclusion

In summary, we developed a two lipid and two-in-one lipid system incorporated with designed glycolipids to form new BLNPs for DC-targeting and adjuvant effect. Using SARS-CoV-2 spike mRNA as the cargo, we evaluated the preferential cellular uptake by DCs, and significant enhancement of humoral immune responses, neutralizing antibodies, and T cell-mediated immune responses. The mRNA-BLNP1 vaccine induced greater levels of cytokines than L3+mRNA alone. After two immunizations, the mRNA-BLNP1 vaccine elicited robust neutralizing antibody responses at significantly higher levels than that induced by the mRNA-LNPs without L3. Based on this study, we expect that the mRNA-GZ-BLNP1, mRNA-IZ-BLNP1 or mRNA-LNP vaccine containing L3 would be valuable in aiding the fight against infectious diseases. In addition, we have demonstrated that the spike mRNA-GZ-BLNP1 vaccine with deletion of glycosites in the stem (CD/HR2) to expose the conserved epitopes provided a better protection against SARS-CoV-2 variants as compared to the mRNA-GZ-LNP vaccine.

ASSOCIATED CONTENT

Supporting Information.

The Supporting Information is available free of charge at __.

AUTHOR INFORMATION

Corresponding Author

Chi-Huey Wong − Genomics Research Center, Academia Sinica, Taipei 115, Taiwan; Department of Chemistry, The Scripps Research Institute, La Jolla, California 92037, United States; orcid.org/0000-0002-9961-7865; Email: wong@scripps.edu.tw

Authors

Chen-Yo Fan − Genomics Research Center, Academia Sinica, Taipei 115, Taiwan

Szu-Wen Wang − Genomics Research Center, Academia Sinica, Taipei 115, Taiwan

Jia-Yan Chen − Genomics Research Center, Academia Sinica, Taipei 115, Taiwan

Notes

The authors declare no competing financial interest.

ACKNOWLEDGMENT

This research was supported by Academia Sinica. We thank the National RNAi Core Facility at Academia Sinica for pseudotyped Lentivirus neutralization assay and related services.

REFERENCES

1. Zhao, J.; Zhao, S.; Ou, J.; Zhang, J.; Lan, W.; Guan, W.; Wu, X.; Yan, Y.; Zhao, W.; Wu, J.; Chodosh, J.; Zhang, Q., COVID-19: Coronavirus Vaccine Development Updates. *Front. Immunol.* **2020,** *11*.
2. Alberer, M.; Gnad-Vogt, U.; Hong, H. S.; Mehr, K. T.; Backert, L.; Finak, G.; Gottardo, R.; Bica, M. A.; Garofano, A.; Koch, S. D.; Fotin-Mleczek, M.; Hoerr, I.; Clemens, R.; von Sonnenburg, F., Safety and immunogenicity of a mRNA rabies vaccine in healthy adults: an open-label, non-randomised, prospective, first-in-human

phase 1 clinical trial. *The Lancet* **2017,** *390* (10101), 1511-1520.
3. Feldman, R. A.; Fuhr, R.; Smolenov, I.; Ribeiro, A.; Panther, L.; Watson, M.; Senn, J. J.; Smith, M.; Almarsson, Ö.; Pujar, H. S.; Laska, M. E.; Thompson, J.; Zaks, T.; Ciaramella, G., mRNA vaccines against H10N8 and H7N9 influenza viruses of pandemic potential are immunogenic and well tolerated in healthy adults in phase 1 randomized clinical trials. *Vaccine* **2019,** *37* (25), 3326-3334.
4. Anderson, E. J.; Rouphael, N. G.; Widge, A. T.; Jackson, L. A.; Roberts, P. C.; Makhene, M.; Chappell, J. D.; Denison, M. R.; Stevens, L. J.; Pruijssers, A. J.; McDermott, A. B.; Flach, B.; Lin, B. C.; Doria-Rose, N. A.; O'Dell, S.; Schmidt, S. D.; Corbett, K. S.; Swanson, P. A.; Padilla, M.; Neuzil, K. M.; Bennett, H.; Leav, B.; Makowski, M.; Albert, J.; Cross, K.; Edara, V. V.; Floyd, K.; Suthar, M. S.; Martinez, D. R.; Baric, R.; Buchanan, W.; Luke, C. J.; Phadke, V. K.; Rostad, C. A.; Ledgerwood, J. E.; Graham, B. S.; Beigel, J. H., Safety and Immunogenicity of SARS-CoV-2 mRNA-1273 Vaccine in Older Adults. *New Engl. J. Med.* **2020,** *383* (25), 2427-2438.
5. Walsh, E. E.; Frenck, R. W.; Falsey, A. R.; Kitchin, N.; Absalon, J.; Gurtman, A.; Lockhart, S.; Neuzil, K.; Mulligan, M. J.; Bailey, R.; Swanson, K. A.; Li, P.; Koury, K.; Kalina, W.; Cooper, D.; Fontes-Garfias, C.; Shi, P.-Y.; Türeci, Ö.; Tompkins, K. R.; Lyke, K. E.; Raabe, V.; Dormitzer, P. R.; Jansen, K. U.; Şahin, U.; Gruber, W. C., Safety and Immunogenicity of Two RNA-Based Covid-19 Vaccine Candidates. *New Engl. J. Med.* **2020,** *383* (25), 2439-2450.
6. Zhang, Y.; Sun, C.; Wang, C.; Jankovic, K. E.; Dong, Y., Lipids and Lipid Derivatives for RNA Delivery. *Chem. Rev.* **2021,** *121* (20), 12181-12277.
7. Pardi, N.; Hogan, M. J.; Porter, F. W.; Weissman, D., mRNA vaccines — a new era in vaccinology. *Nature Reviews Drug Discovery* **2018,** *17* (4), 261-279.
8. Sahin, U.; Karikó, K.; Türeci, Ö., mRNA-based therapeutics — developing a new class of drugs. *Nature Reviews Drug Discovery* **2014,** *13* (10), 759-780.
9. Islam, M. A.; Reesor, E. K. G.; Xu, Y.; Zope, H. R.; Zetter, B. R.; Shi, J., Biomaterials for mRNA delivery. *Biomaterials Science* **2015,** *3* (12), 1519-1533.
10. Ramaswamy, S.; Tonnu, N.; Tachikawa, K.; Limphong, P.; Vega, J. B.; Karmali, P. P.; Chivukula, P.; Verma, I. M., Systemic delivery of factor IX messenger RNA for protein replacement therapy. *Proceedings of the National Academy of Sciences* **2017,** *114* (10), E1941-E1950.
11. Kauffman, K. J.; Dorkin, J. R.; Yang, J. H.; Heartlein, M. W.; DeRosa, F.; Mir, F. F.; Fenton, O. S.; Anderson, D. G., Optimization of Lipid Nanoparticle Formulations for mRNA Delivery in Vivo with Fractional Factorial and Definitive Screening Designs. *Nano Lett.* **2015,** *15* (11), 7300-7306.
12. Yanez Arteta, M.; Kjellman, T.; Bartesaghi, S.; Wallin, S.; Wu, X.; Kvist, A. J.; Dabkowska, A.; Székely, N.; Radulescu, A.; Bergenholtz, J.; Lindfors, L., Successful reprogramming of cellular protein production through mRNA delivered by functionalized lipid nanoparticles. *Proceedings of the National Academy of Sciences* **2018,** *115* (15), E3351-E3360.
13. McKinlay, C. J.; Vargas, J. R.; Blake, T. R.; Hardy, J. W.; Kanada, M.; Contag, C. H.; Wender, P. A.; Waymouth, R. M., Charge-altering releasable transporters (CARTs) for the delivery and release of mRNA in living animals. *Proceedings of the National Academy of Sciences* **2017,** *114* (4), E448-E456.
14. Oberli, M. A.; Reichmuth, A. M.; Dorkin, J. R.; Mitchell, M. J.; Fenton, O. S.; Jaklenec, A.; Anderson, D. G.; Langer, R.; Blankschtein, D., Lipid Nanoparticle Assisted mRNA Delivery for Potent Cancer Immunotherapy. *Nano Lett.* **2017,** *17* (3), 1326-1335.
15. Capasso Palmiero, U.; Kaczmarek, J. C.; Fenton, O. S.; Anderson, D. G., Poly(β-amino ester)-co-poly(caprolactone) Terpolymers as Nonviral Vectors for mRNA Delivery In Vitro and In Vivo. *Advanced Healthcare Materials* **2018,** *7* (14), 1800249.
16. Tam, H. H.; Melo, M. B.; Kang, M.; Pelet, J. M.; Ruda, V. M.; Foley, M. H.; Hu, J. K.; Kumari, S.; Crampton, J.; Baldeon, A. D.;

Sanders, R. W.; Moore, J. P.; Crotty, S.; Langer, R.; Anderson, D. G.; Chakraborty, A. K.; Irvine, D. J., Sustained antigen availability during germinal center initiation enhances antibody responses to vaccination. **2016,** *113* (43), E6639-E6648.
17. White, K. L.; Rades, T.; Furneaux, R. H.; Tyler, P. C.; Hook, S., Mannosylated liposomes as antigen delivery vehicles for targeting to dendritic cells†. *J. Pharm. Pharmacol.* **2006,** *58* (6), 729-737.
18. Wolff, J. A.; Malone, R. W.; Williams, P.; Chong, W.; Acsadi, G.; Jani, A.; Felgner, P. L., Direct Gene Transfer into Mouse Muscle in Vivo. *Science* **1990,** *247* (4949), 1465-1468.
19. Lazzaro, S.; Giovani, C.; Mangiavacchi, S.; Magini, D.; Maione, D.; Baudner, B.; Geall, A. J.; De Gregorio, E.; D'Oro, U.; Buonsanti, C., CD8 T-cell priming upon mRNA vaccination is restricted to bone-marrow-derived antigen-presenting cells and may involve antigen transfer from myocytes. *Immunology* **2015,** *146* (2), 312-326.
20. Geall, A. J.; Mandl, C. W.; Ulmer, J. B., RNA: The new revolution in nucleic acid vaccines. *Semin. Immunol.* **2013,** *25* (2), 152-159.
21. Wu, T.-N.; Lin, K.-H.; Chang, Y.-J.; Huang, J.-R.; Cheng, J.-Y.; Yu, A. L.; Wong, C.-H., Avidity of CD1d-ligand-receptor ternary complex contributes to T-helper 1 (Th1) polarization and anticancer efficacy. *Proceedings of the National Academy of Sciences* **2011,** *108* (42), 17275-17280.
22. Brennan, P. J.; Brigl, M.; Brenner, M. B., Invariant natural killer T cells: an innate activation scheme linked to diverse effector functions. *Nature Reviews Immunology* **2013,** *13* (2), 101-117.
23. Dölen, Y.; Kreutz, M.; Gileadi, U.; Tel, J.; Vasaturo, A.; van Dinther, E. A. W.; van Hout-Kuijer, M. A.; Cerundolo, V.; Figdor, C. G., Co-delivery of PLGA encapsulated invariant NKT cell agonist with antigenic protein induce strong T cell-mediated antitumor immune responses. *Oncoimmunology* **2016,** *5* (1), e1068493.
24. Ghinnagow, R.; De Meester, J.; Cruz, L. J.; Aspord, C.; Corgnac, S.; Macho-Fernandez, E.; Soulard, D.; Fontaine, J.; Chaperot, L.; Charles, J.; Soncin, F.; Mami-Chouaib, F.; Plumas, J.; Faveeuw, C.; Trottein, F., Co-delivery of the NKT agonist α-galactosylceramide and tumor antigens to cross-priming dendritic cells breaks tolerance to self-antigens and promotes antitumor responses. *Oncoimmunology* **2017,** *6* (9), e1339855.
25. Macho-Fernandez, E.; Cruz, L. J.; Ghinnagow, R.; Fontaine, J.; Bialecki, E.; Frisch, B.; Trottein, F.; Faveeuw, C., Targeted Delivery of α-Galactosylceramide to CD8α+ Dendritic Cells Optimizes Type I NKT Cell–Based Antitumor Responses. *The Journal of Immunology* **2014,** *193* (2), 961-969.
26. Thapa, P.; Zhang, G.; Xia, C.; Gelbard, A.; Overwijk, W. W.; Liu, C.; Hwu, P.; Chang, D. Z.; Courtney, A.; Sastry, J. K.; Wang, P. G.; Li, C.; Zhou, D., Nanoparticle formulated alpha-galactosylceramide activates NKT cells without inducing anergy. *Vaccine* **2009,** *27* (25), 3484-3488.
27. Fujio, M.; Wu, D.; Garcia-Navarro, R.; Ho, D. D.; Tsuji, M.; Wong, C.-H., Structure-Based Discovery of Glycolipids for CD1d-Mediated NKT Cell Activation: Tuning the Adjuvant versus Immunosuppression Activity. *J. Am. Chem. Soc.* **2006,** *128* (28), 9022-9023.
28. Wu, T.-N.; Lin, K.-H.; Wu, Y.-T.; Huang, J.-R.; Hung, J.-T.; Wu, J.-C.; Chen, C.-Y.; Chu, K.-C.; Lin, N.-H.; Yu, A. L.; Wong, C.-H., Phenyl Glycolipids with Different Glycosyl Groups Exhibit Marked Differences in Murine and Human iNKT Cell Activation. *ACS Chem. Biol.* **2016,** *11* (12), 3431-3441.
29. Semple, S. C.; Akinc, A.; Chen, J.; Sandhu, A. P.; Mui, B. L.; Cho, C. K.; Sah, D. W. Y.; Stebbing, D.; Crosley, E. J.; Yaworski, E.; Hafez, I. M.; Dorkin, J. R.; Qin, J.; Lam, K.; Rajeev, K. G.; Wong, K. F.; Jeffs, L. B.; Nechev, L.; Eisenhardt, M. L.; Jayaraman, M.; Kazem, M.; Maier, M. A.; Srinivasulu, M.; Weinstein, M. J.; Chen, Q.; Alvarez, R.; Barros, S. A.; De, S.; Klimuk, S. K.; Borland, T.; Kosovrasti, V.; Cantley, W. L.; Tam, Y. K.; Manoharan, M.; Ciufolini, M. A.; Tracy, M. A.; de Fougerolles, A.; MacLachlan, I.; Cullis, P. R.; Madden, T. D.; Hope, M. J., Rational

design of cationic lipids for siRNA delivery. *Nat. Biotechnol.* **2010,** *28* (2), 172-176.
30. Wasungu, L.; Hoekstra, D., Cationic lipids, lipoplexes and intracellular delivery of genes. *Journal of Controlled Release* **2006,** *116* (2), 255-264.
31. Cheng, X.; Lee, R. J., The role of helper lipids in lipid nanoparticles (LNPs) designed for oligonucleotide delivery. *Adv. Drug Del. Rev.* **2016,** *99*, 129-137.
32. Tros de Ilarduya, C.; Sun, Y.; Düzgüneş, N., Gene delivery by lipoplexes and polyplexes. *Eur. J. Pharm. Sci.* **2010,** *40* (3), 159-170.
33. Vaidyanathan, S.; Orr, B. G.; Banaszak Holl, M. M., Role of Cell Membrane–Vector Interactions in Successful Gene Delivery. *Acc. Chem. Res.* **2016,** *49* (8), 1486-1493.
34. Liu, S.; Wang, X.; Yu, X.; Cheng, Q.; Johnson, L. T.; Chatterjee, S.; Zhang, D.; Lee, S. M.; Sun, Y.; Lin, T.-C.; Liu, J. L.; Siegwart, D. J., Zwitterionic Phospholipidation of Cationic Polymers Facilitates Systemic mRNA Delivery to Spleen and Lymph Nodes. *J. Am. Chem. Soc.* **2021,** *143* (50), 21321-21330.

Supplementary Information

Materials and Methods

For chemical synthesis, all starting materials and commercially obtained reagents were purchased from Sigma-Aldrich and used as received unless otherwise noted. All reactions were performed in oven-dried glassware under nitrogen atmosphere using dry solvents. Silica gel (E, Merck) was used for flash chromatography. Transmission electron microscopy (TEM) images were obtained by a FEI Tecnai G2 F20 S-Twin. EM imaging was conducted in bright-field mode at an operating voltage of 200 kV. Images were recorded at a defocus value of ~1.8 μm under low-dose exposures (25–30 e/Å2) with a 4k × 4k charge-coupled device camera (Glatan, Pleasanton, CA, USA) at a magnification of 50,000×. Experiments were carried out at the Academia Sinica Cryo-EM Facility (Taipei, Taiwan). mMESSAGE mMACHINE® Kit and SYBR™ Safe DNA Gel Stain is from Thermo Scientific™. 18:1 PE CF and DMG-PEG2000 are from Avanti Polar Lipids, Inc. Cholesterol and DSPC are from Sigma Aldrich. SM-102 is from MedChemExpress. IFNγ and IL-4 ELISpot kit are from Mabtech AB.

Experimental Section

Cell Cultures

Human Embryonic Kidney Cells 293 (HEK293T cell) was cultured in Dulbecco's modified Eagle's medium (DMEM) (invitrogen, Carlsbad, CA, USA) supplemented with 10% fetal bovine serum (FBS) (Invitrogen) and 1% Gibco Antibiotic-Antimycotic (anti-anti) (Invitrogen).

Animals

Balb/c mice (8 weeks) were purchased from National Laboratory Animal Center, Taiwan. All the mice were maintained in a specific pathogen-free environment. Eight-week-old Balb/c mice were immunized i.m. twice with 2-week interval. Each vaccination contains in PBS (100 μl). Sera collected from immunized mice were subjected to ELISA analysis 10 days after the last immunization. The experimental protocol was approved by Academia Sinica's Institutional Animal Care and Utilization Committee (approval no. 22-08-1901).

Antibodies and Proteins

The SARS-CoV-2 full-length spike protein was purchased from ACROBiosystems. HRP conjugated anti-mouse secondary antibody and horseradish peroxidase substrate were purchased

from Thermo Scientific. Mouse monoclonal anti–β-actin were purchased from Millipore. All commercial antibodies were validated for specificity by companies via Western blot.

Construction of mRNA synthesis plasmid

The DNA sequence of WT (Wuhan/WH01/2019 strain) SARS-CoV-2 spike (1-1273) with K986P and K987P mutation (2P) were codon-optimized for Homo sapiens. The spike DNA sequence was cloned into pMRNAXP mRNA Synthesis Vector (System Biosciences) that contains T7 promoter, 5' and 3' UTR and poly A tail. Briefly, pMRNAXP vector was digested with EcoRI and BamHI (Thermo Scientific™) at 37°C for 1 hour. DNA sequence of the spike protein were amplified by KOD OneTM PCR master mix (TOYOBO Bio-Technology). The linearized pMRNAXP vector and the PCR fragments of DNA encoding spike were cleaned up by Wizard® SV Gel and PCR Clean-Up System (Promega). The PCR fragments of spike protein DNA were cloned into linearized pMRNAXP vector using In-Fusion® HD Cloning Kit (Clontech® Laboratories, Inc.). The cloning mixtures were transformed to One Shot™ TOP10 Chemically Competent E. coli (Thermo Scientific™) and incubated at 37°C overnight.

In vitro transcription of mRNA

mRNA was produced using mMESSAGE mMACHINE® Kit (Thermo Scientific™) according to the user guide. Briefly, DNA was linearized by NdeI (Thermo Scientific™) downstream of the poly A tail at 37°C for 1 hour and cleaned up. The linearized DNA was in vitro-transcribed using T7 RNA polymerase in the presence of cap analog [m7G(5')ppp(5')G] and NTP at 37°C for 2 hours. DNase was added to the mixture and incubated at 37°C for 15 minutes to digest double-stranded DNA. mRNA was precipitated by lithium chloride (LiCl) and the mixture were centrifuged to remove unincorporated nucleotides and protein. The mRNA pellet was washed with 70% ethanol and re-centrifuged to remove remaining unincorporated nucleotides. The mRNA was resuspended in nuclease-free water and stored at -20°C until use.

Fabrication of mRNA lipid nanoparticles

The composition of lipids including SM-102, DMG-PEG2000, DSPC (1,2-distearoyl-sn-glycero-3-phosphocholine), cholesterol and DMG-PEG2000 were prepared in ethanol at a molar ratio of 50:10:38.5:1.5. mRNA was dissolved in 10 mM pH 4 citric acid buffer. The weight ratio of lipid: mRNA was 3:1 and the nitrogen-to-phosphate (N/P) ratio was 3. For syringe injection, organic phase and aqueous phase were injected via syringes simultaneously. The mixture was then diluted 2 times with PBS. For microfluidic device, organic phase and aqueous phase were passed through the channel on the cartridge using NanoAssemblr® Ignite™ (Precision NanoSystems) and the mixture were then diluted 2 times with PBS. The flow rate ratio (FRR) (aqueous phase and organic phase) was 6. The formed mRNA-LNP was dialyzed against PBS by MWCO 3.5 kDa dialysis membrane (SPECTRUMLABS®.COM)

Quantification of encapsulated mRNA

Encapsulation efficiency was determined by Quant-iTTM RiboGreenTM RNA Reagent and Kit (Thermo Scientific™). Samples were diluted 250-fold with 1X TE buffer and further diluted 2-fold with TE buffer or TE buffer containing 2% Triton X-100. Ribosomal mRNAs were prepared as 100, 50, 25, 12.5 and 0 ng/ml in TE or TE buffer containing 1% Triton X-100 to establish the standard curve. After incubation at 37 ºC for 10 minutes, Quant-iTTM RiboGreenTM RNA Reagent was added into well. The fluorescence intensity was measured by CLARIOstar® Plus (BMG Labtech).

Cell culture

Human Embryonic Kidney Cells 293 (HEK293T cell) were cultured in Dulbecco's modified Eagle's medium (DMEM) (Thermo Scientific™) supplemented with 10% fetal bovine serum (FBS) (Thermo Scientific™) and 1% Gibco™ Antibiotic-Antimycotic (anti-anti) (Thermo Scientific™).

HEK293T cell transfection

HEK293T cells were plated at $5*10^5$ cells per well in a 6-well plate in 2.5 mL DMEM media. 1 μg of the GFP mRNA was formulated with the corresponding LNP by the procedure mentioned above and then added to the cells. 24 h post-transfection, GFP expression was monitored by fluorescence microscopy.

Splenic cells preparation and BMDCs culture

To prepare splenic cells, mouse spleen was homogenized with the frosted end of glass slide, treated with RBC lysis buffer (Sigma) to deplete red blood cells (RBCs), followed by passing through the cell strainer (BD Biosciences). Bone-marrow derived dendritic cells (BMDCs) were prepared as described.[3] Briefly, bone marrow was isolated from mouse femurs and tibiae and treated with RBC lysis buffer (Sigma-Aldrich) to deplete RBCs. Cells were then cultured in RPMI-1640 containing 10% heat inactivated FBS (Thermo Fisher Scientific), 1% Penicillin/Streptomycin (Thermo Fisher Scientific), 50 μM 2-mercaptoethanol (Thermo Fisher Scientific), and 20 ng/ml recombinant mouse GM-CSF (eBioscience) at a density of 2×10^5 cells/ml. The cells were supplemented with an equal volume of the complete culture medium described above at day 3 and refreshed with one-half the volume of medium at day 6. At day 8, the suspended cells were then harvested.

Treatment of LNPs to splenic cells and BMDCs

Splenic cells or BMDCs were incubated with different FITC-labeled LNP formulations (1 μg/mL) (mRNA-LNP, mRNA-BLNP1, and mRNA-BLNP2) in RPMI-1640 at 37 ℃ for 1 hours. Cells were blocked with Fc receptor binding inhibitor (clone: 93, eBioscience) for 20 minutes. Splenocytes were stained with antibodies against CD3 (clone: 17A2, BV421-conjugated, Biolegend), CD19 (clone: 1D3, PECy7-conjugated, BD Biosciences). BMDCs were stained with antibody against CD11c (clone N418 APC-conjugated, Biolegend). Labeled cells were analyzed using FACSC and Flow Cytometer (BD Biosciences).

Flow Cytometry

After incubation with different mRNA-LNPs, BMDC cells were washed with ice-cold FACS buffer (1% FBS in 1 × DPBS with 0.1% Sodium Azide), and incubated with purified anti-mouse CD16/32 antibody (BioLegend) in FACS buffer on ice for 20 min, followed by washing with FACS buffer. BMDCs were stained with APC anti-mouse CD11c antibody (BioLengend) at 4℃ for 30 min, and washed with FACS buffer. Finally, BMDCs were stained with propidium iodide (Sigma-Aldrich). Flow cytometry was performed on FACSCanto flow cytometer (BD Bioscience).

Animal Immunizations

BALB/c mice aged 6 to 8 wk old (n = 5) were immunized intramuscularly with 15 μg of mRNA-LNPs in phosphate-buffered saline (PBS). Animals were immunized at wk 0 and boosted with a second vaccination at wk 2, and serum samples were collected from each mouse 1 wk after the second immunization.

Measurement of serum IgG titer

ELISA was used to determine the IgG titer of the mouse serum. The wells of a 96-well ELISA plate (Greiner Bio-One) were coated with 100 ng SARS-CoV-2 spike protein (ACROBiosystems) in 100mM sodium bicarbonate pH 8.8 at 4°C overnight. The wells were blocked with 200 ul 5% skim milk in 1X PBS at 37 °C for 1 hour and washed with 200 ul PBST (1X PBS, 0.05% Tween 20, pH 7.4) three times. Mice serum samples with 2-fold serial dilution were added into wells for an incubation at 37 °C for 2 hours and washed with 200 ul PBST six times. The wells were incubated with 100 ul HRP conjugated anti-mouse secondary antibody (1:10000, in PBS) at 37 °C for 1 hour and washed with 200 ul PBST six times. 100 µl horseradish peroxidase substrate (1-Step™ Ultra TMB-ELISA Substrate Solution) (Thermo Scientific™) was added into wells followed by 100 ul 1M H_2SO_4. After incubation for 30 mins, Absorbance (OD 450 nm) was measured by SpectraMax M5.

Pseudovirus neutralization assay

Pseudovirus was constructed by the RNAi Core Facility at Academia Sinica using a procedure similar to that described previously.[4] Briefly, the pseudotyped lentivirus carrying SARS-CoV-2 spike protein was generated by transiently transfecting HEK-293T cells with pCMV-ΔR8.91, pLAS2w.Fluc.Ppuro. HEK-293T cells were seeded one day before transfection, and indicated plasmids were delivery into cells by using TransITR-LT1 transfection reagent (Mirus). The culture medium was refreshed at 16 hr and harvested at 48 hr and 72hr post-transfection. Cell debris was removed by centrifugation at 4,000 xg for 10 min, and the supernatant was passed through 0.45-µm syringe filter (Pall Corporation). The pseudotyped lentivirus was aliquot and then stored at -80°C. To estimate the lentiviral titer by AlarmaBlue assay (Thermo Scientific), The transduction unit (TU) of SARS-CoV-2 pseudotyped lentivirus was estimated by using cell viability assay in responded to the limited dilution of lentivirus. In brief, HEK-293T cells stably expressing human ACE2 gene were plated on 96-well plate one day before lentivirus transduction. For the titering pseudotyped lentivirus, different amounts of lentivirus were added into the culture medium containing polybrene (final concentration 8 µg/ml). Spin infection was carried out at 1,100 xg in 96-well plate for 30 minutes at 37 °C. After incubating cells at 37°C for 16 hr, the culture medium containing virus and polybrene were removed and replaced with fresh complete DMEM containing 2.5 µg/ml puromycin. After treating puromycin for 48 hrs, the culture media was removed and the cell viability was detected by using 10% AlamarBlue reagents according to manufacturer's instruction. The survival rate of uninfected cells (without puromycin treatment) was set as 100%. The virus titer (transduction units) was determined by plotting the survival cells versus diluted viral dose. For neutralization assay, heat-inactivated sera or antibodies were serially diluted and incubated with 1,000 TU of SARS-CoV-2 pseudotyped lentivirus in DMEM for 1 h at 37°C. The mixture was then inoculated with 10,000 HEK-293T cells stably expressing human ACE2 gene in a 96-well plate. The culture medium was replaced with fresh complete DMEM (supplemented with 10% FBS and 100 U/mL penicillin/streptomycin) at 16 h postinfection and continuously cultured for another 48 h. The expression level of luciferase gene was determined by using Bright-Glo Luciferase Assay System (Promega). The relative light unit (RLU) was detected by Tecan i-control (Infinite 500). The percentage of inhibition was calculated as the ratio of RLU reduction in the presence of diluted serum to the RLU value of no serum control using the formula ($RLU^{control}$ - RLU^{Serum})/RLU control.

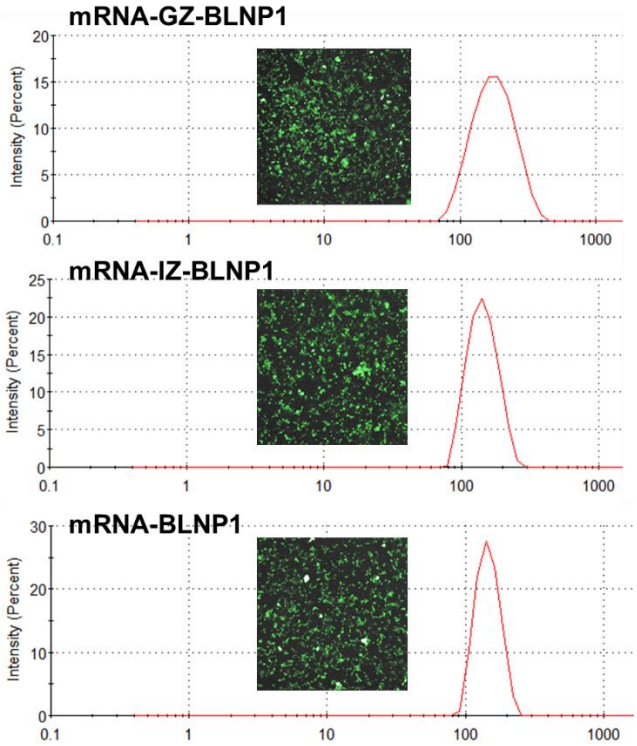

Figure S1. Size distribution and image of GFP-encoding mRNA in HEK-293T cell of mRNA-GZ-BLNP1, mRNA-IZ-BLNP1 and mRNA-BLNP1, respectively.

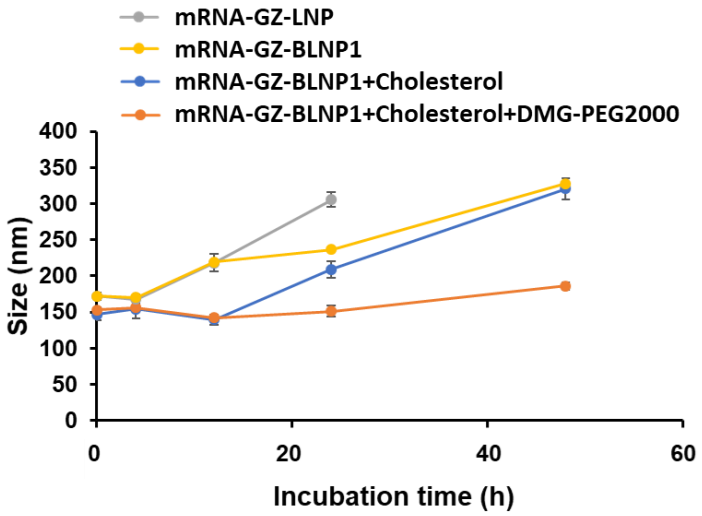

Figure S2. Size variation of different LNP formulation in 10% FBS solution at different incubation time.

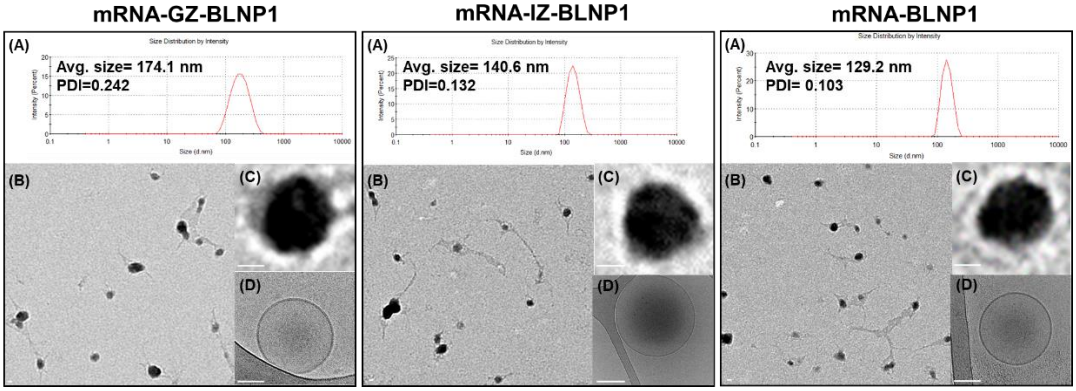

Figure S3. (A) Size distribution (B) TEM image (C) enlarged TEM image (D) enlarged CryoEM image of mRNA-GZ-BLNP1, mRNA-IZ-BLNP1, and mRNA-BLNP1. White scale bar represents 50 nm.

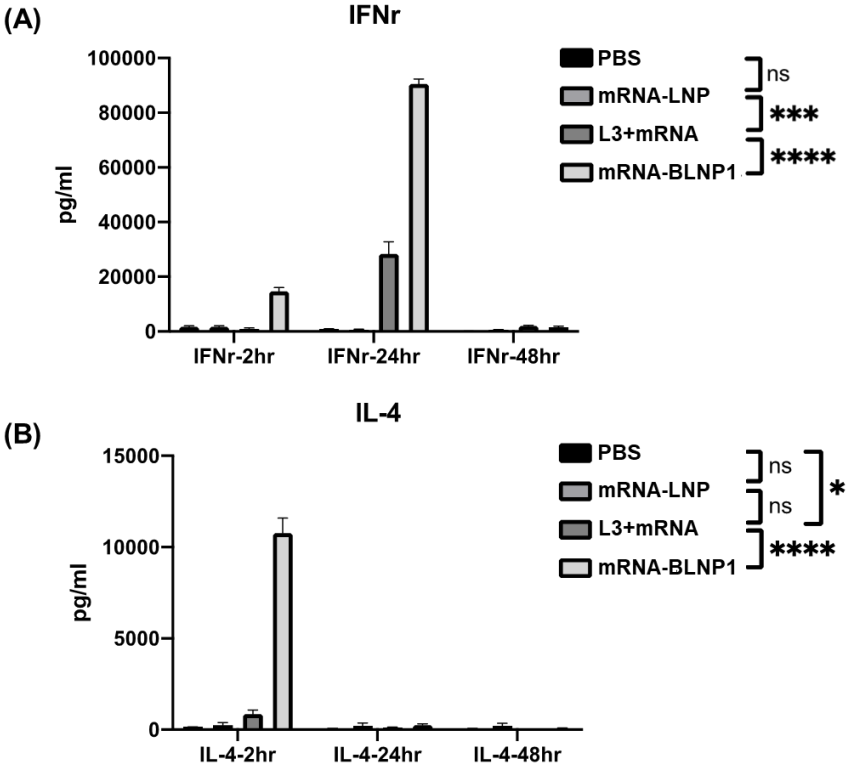

Figure S4. The humoral immune response induced by different conformation of LNPs. (A) IFN-γ induced by mRNA-LNP, L3+mRNA, or mRNA-BLNP1 (B) IL-4 induced by mRNA-LNP, mRNA-L3 or mRNA-BLNP1. Cytokines were analyzed in mice serum at 2, 24, or 48 h after immunization.

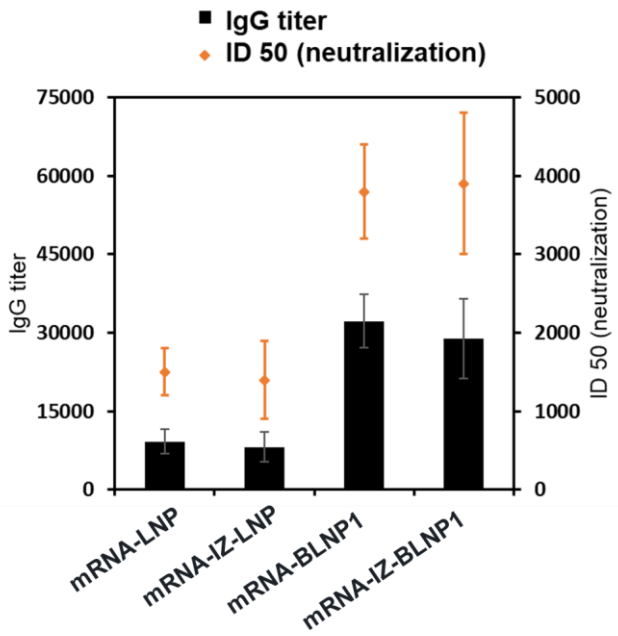

Figure S5. IgG titer and pseudovirus-based neutralization assay of mRNA-LNP, mRNA-IZ-LNP, mRNA-BLNP1 and mRNA-IZ-BLNP1. Mice were immunized with at day 0 and day 14 and the serum were collected at day 21.